DROP TESTING OF BIODEGRADABLE PLASTICS FOR CONSUMER PRODUCT APPLICATIONS

Nagi Elabbasi, David J. Quinn, Glenn Bergevin, and Lindsay H. Landry

Veryst Engineering, Needham, MA, USA

THEME

Material Characterisation

KEYWORDS

Biodegradable polymers, constitutive modelling, drop test, polymer modelling.

SUMMARY

Biodegradable plastics are becoming increasingly attractive for consumer product applications such as electronic devices and disposable packaging. There is therefore an increasing need to accurately model and simulate bioplastic product performance to provide design insight. The mechanical behaviour of bioplastics is traditionally assumed to be linear elastic, hyperelastic or linear viscoelastic. However, these constitutive models do not accurately capture the viscous flow and strain rate effects necessary for accurate evaluation of impact resistance. In this work, the shortcomings of these traditional material models are illustrated in the context of drop testing. A material model for biodegradable plastics is developed which accounts for hyperelastic, nonlinear viscous flow and strain rate effects. The material model is based on the Parallel Network model included in Veryst Engineering's PolyUMod software. The experimental test data required to accurately calibrate the material model are discussed, and models for two different biodegradable materials are calibrated. The material models are used to analyze the drop test performance of a biodegradable plastic protective case for a generic smart phone. A nonlinear, explicit transient dynamic finite element analysis is performed, and the effect of the case material model on the peak strains, energy dissipation, and transmitted forces is evaluated. This combination of a calibrated advanced material model and nonlinear finite element analysis constitute a valuable tool for consumer drop testing applications, especially early in the design process.

DROP TESTING OF BIODEGRADABLE PLASTICS FOR CONSUMER PRODUCT APPLICATIONS

1: Introduction

The finite element method is frequently used to simulate consumer product drop tests. These FEM simulations can help designers identify problems early in the design process, when the cost associated with redesign is low. The reliability of numerical predictions is dependent on the accuracy of the finite element model, including the material constitutive behaviour at high strains and strain rates. As new classes of materials are developed, there is an increased need for advanced constitutive models to capture unique material characteristics, such as severe nonlinearities and rate-dependent dissipative characteristics.

One class of materials that has received significant attention in recent years is biodegradable plastics. The most common bioplastics are those derived from poly-lactic acid (PLA). PLA-derived materials have found applications in disposable packaging, implantable medical devices, and, most notably for this work, consumer electronics. The first generation of these materials was comprised mainly of pure PLA, or poly-L-lactide (PLLA), which is typically a relatively stiff, brittle material with a Young's modulus and failure strain ranging from 1-3.6 GPa and 2-4%, respectively. The variability in PLA's mechanical properties depends on several factors including molecular weight, degree of crystallinity, material processing and material degradation. However more recently there have been efforts aimed at including additives in PLA-derived materials, such as natural and synthetic fibers for increased strength, or plasticizers for increased ductility and energy dissipation (Graupner, et al., 2009; Martin and Avérouz, 2001). For such materials, the typical linear elastic or linear viscoelastic constitutive models are insufficient for characterizing the appropriate material behaviour for a number of applications, including impact resistance, which is particularly relevant for drop testing.

In this work, we establish a framework for appropriately modelling different variations of biodegradable plastics for drop testing applications. After a brief discussion of the mechanical behaviours of both a standard and chemically-enhanced biodegradable material, we present an advanced constitutive model capable of capturing the salient behaviour of biodegradable plastics for use in consumer electronic applications. The application of this material model is then demonstrated through the simulation of a drop test of a protective case for a generic smart phone. Results of this drop test for a linear-viscoelastic material model are compared to the advanced model using standard performance metrics such as maximum principal strain, energy dissipation and force transmission. Finally, we discuss further improvements to our material model that can in the future lead to more accurate simulation results.

2: Mechanical Behaviour of Biodegradable Plastics

The mechanical responses of a pure and a plasticized PLA material subjected to uniaxial tension are compared in Figures 1 and 2, respectively. Figure 1 illustrates the rate-dependent loading-unloading response of a pure PLA currently in use for a protective phone case application. Generally speaking, this material, subsequently referred to as “Material 1”, exhibits an initially linear response during loading with moderate energy dissipation during unloading cycles, followed by brittle failure at a strain and stress of 2.5-3.5% and ~35MPa, respectively. Material 1 exhibits mild rate-sensitivity over an order of magnitude change in strain rate. The plasticized material shown in Figure 2, subsequently referred to as “Material 2”, however, exhibits significant rate dependence across the three loading rates examined and significantly more ductility with failure strains ranging from 20-90%. This represents a significant increase in failure strain with minimal change in failure stress, a combination of characteristics which may be of particular interest for applications requiring enhanced energy dissipation.

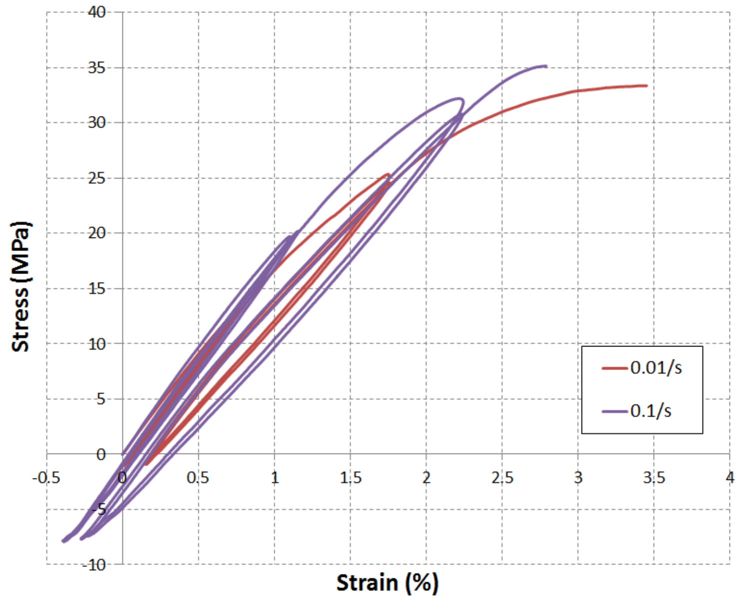

Figure 1: Engineering stress-strain curves for Material 1 (a pure PLA) subjected to uniaxial tension load-unload cycles at two strain rates.

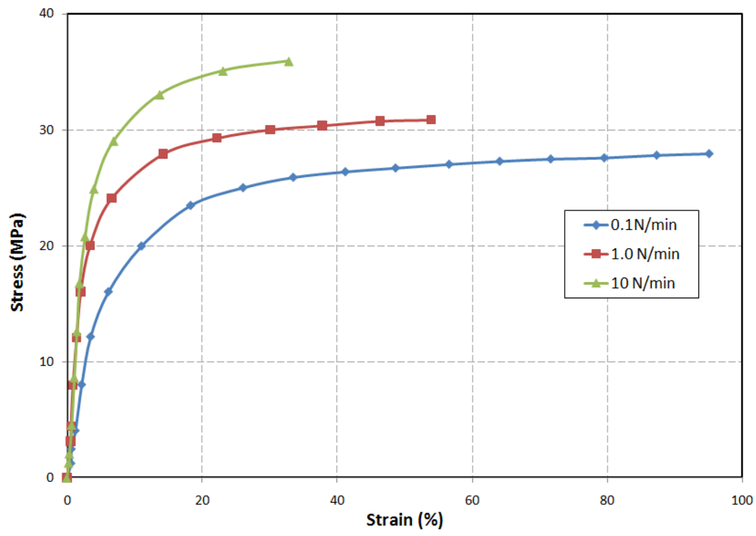

Figure 2: Engineering stress-strain curves for Material 2 (plasticized PLLA) at three loading rates. Data from Grabow et al. (2005).

3: Material Model

In this section we develop a material model for the two biodegradable materials discussed above. The stress-strain behaviour of both materials clearly cannot be captured with a linear elastic material model. A hyperelastic material is similarly impractical since it will follow exactly the same path during loading and unloading and not capture any energy dissipation. The energy dissipation and the observed rate dependence may be captured by a linear viscoelastic model. A linear viscoelastic model also captures important behaviours such as creep and stress relaxation. As we show later, linear viscoelasticity is indeed a good choice for Material 1. However, linear viscoelasticity is not suitable for Material 2, where there is significant plastic deformation. Another shortcoming of linear viscoelasticity is that the loss modulus does not depend on amplitude of cyclic strain. This behaviour does not agree with experimental data for plastics (Bergstrom, 2008). For more details on material models suitable for polymers, see Bergstrom and Boyce (1998, 2001).

A literature review of material modelling of biodegradable polymers reveals that most use traditional material models, such as those described in the previous sections, which are not suitable for applications such as drop testing. Soares et al. (2008, 2010) used a hyperelastic material model for PLLA and added viscoelastic effects only to account for the material degradation. Grabow et al. (2002) used a bilinear metal plasticity type material model, which also does not account for viscoelastic dissipation. Grabow et al. (2005) and Ponkala (2009) used viscoelastic material models. More accurate material models accounting for both viscous and hyperelastic effects were used by Soares (2008). However, these models are applicable only to relatively brittle materials such as Material 1.

In this paper, we develop a nonlinear material model that accounts for hyperelastic, viscous flow and strain rate effects, and calibrate it to the two biodegradable plastic materials presented above. The material model is based on the Parallel Network model included in Veryst Engineering's PolyUMod software (Veryst Engineering, 2010), which is implemented as a user material subroutine that interfaces with commercial finite element codes. The rheological representation of the Parallel Network model is shown in Figure 3. All networks are assumed to be subjected to the same deformation gradient, and the total Cauchy stress is the sum of the stress contribution from the networks.

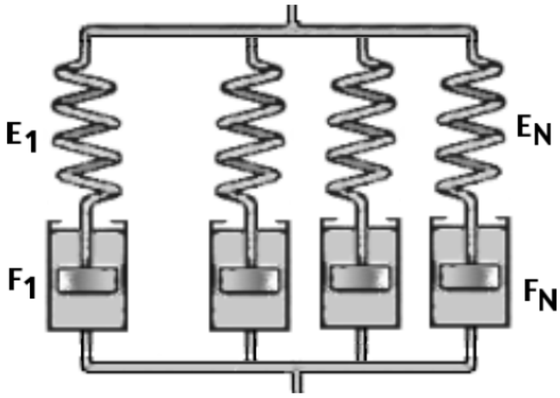

Figure 3: Rheological representation of the general Parallel Network model (Veryst Engineering, 2010)

For both materials three networks are used (N = 3). The first network provides the long term elastic response, including possible damage, and has no viscous effects. Based on the experimental data, the following eight-chain hyperelastic model with a variable shear modulus is used (Veryst Engineering, 2010):

$$\boldsymbol{\sigma}_1 = \frac{\mu_{eff}}{J\overline{\lambda^*}} \frac{L^{-1}(\overline{\lambda^*}/\lambda_L)}{L^{-1}(1/\lambda_L)} \mathrm{dev}[\mathbf{b}^*] + \kappa(J-1)\mathbf{I}, \quad (1)$$

$$\mu_{eff} = \mu_f + (\mu_e - \mu_f)(1 - e^{\frac{-\varepsilon_{eff}}{\overline{\varepsilon}}})\frac{\overline{\varepsilon}}{\varepsilon_{eff}}, \quad (2)$$

where κ is the bulk modulus, J the determinant of the deformation gradient, $\mathbf{b}^*$ is the distortional left Cauchy-Green tensor, $L^{-1}(x)$ is the inverse Langevin function, $\overline{\lambda^*}$ is the chain stretch, and λ_L is the locking stretch. The effective shear modulus μ_{eff} changes with deformation based on the material parameters, μ_f, μ_e, $\overline{\varepsilon}$.

The second network provides the necessary stiffness and damping parameters required to obtain a suitable fit for the low-speed uniaxial stress-strain test data. A standard eight-chain hyperelastic element is used together with a power law viscous damper:

$$\mathbf{D}_2^v = \frac{\dot{\gamma}^P}{\tau} dev[\boldsymbol{\sigma}_2], \tag{3}$$

$$\dot{\gamma}^P = \left(\tau / \bar{\tau}\right)^m \tag{4}$$

where $\mathbf{D}_2^v$ is the viscoplastic flow of Network 2, which is governed by two material parameters $\bar{\tau}, m$. Note that setting parameter *m* equal to one results in a linear viscoelastic damper. However, for many plastics, this parameter is usually higher (Bergstrom and Bischoff, 2010).

The third network is used to obtain a suitable fit for storage and loss moduli at high strain rates and frequencies. A standard eight-chain hyperelastic element is used together with a linear viscoelastic flow component. For many applications where the loading is quasi-static or occurs at low speeds, this third network is not necessary. However, for applications such as drop testing, where high strain rates are to be expected, this network is essential. Note that depending on the application, additional networks may be added to better describe the response for the range of frequencies under consideration.

4: Material Model Calibration

Several tests can be performed to obtain the experimental data necessary to accurately calibrate the material model. For drop testing applications, the response of the material at high and low strains and strain rates are required. The low strain-rate response can be obtained from uniaxial tension tests performed at different strain rates.

Creep and stress relaxation data can also be used to increase the fidelity of the material calibration. However, creep and stress relaxation tests are not sufficient by themselves to capture the hyperelastic part of the deformation. For the high strain rate material parameters, experimental data can be obtained from high-speed uniaxial stress strain testing, forced vibration testing methods such as Direct Mechanical Analysis (DMA), or wave propagation methods, depending on the frequency range. DMA testing covers a wide range of frequencies and account for the effect of mean strain and strain amplitude on the storage and loss moduli.

For this study, low strain/strain rate, creep, and stress relaxation data were gathered for both materials either by direct testing or by using data available in Grabow et al. (2005). No high strain rate test data was gathered for the materials considered in this study. As a result, representative values for standard polymers were used.

The specification of model parameters was performed using MCalibration software, from Veryst Engineering, which uses a Nelder-Mead Simplex optimization algorithm to adjust model parameters to fit experimental data. The normalized mean absolute difference between the experimental data and the material model predictions is used as the fitness function for the optimization. Two calibrations were performed for each material: (1) linear viscoelastic dampers with Neo-Hookean hyperelastic elements, and (2) the three-network model described earlier. Note that for both material models, the third network, responsible for high strain rate effects does not influence the stress-strain predictions at the relatively low strain rates experienced in the uniaxial tension tests, and is therefore calibrated independently based on the specified high frequency storage and loss moduli.

Figure 4 shows a comparison between the model predictions and the experimental data for Material 1. Both the 3-Network model and the viscoelastic model fit the experimental data fairly well. The Parallel Network parameters identified indicate that the viscous strain rate is linearly proportional to stress, (parameter *m* of Eqn. 4 approximately equal to 1.0).

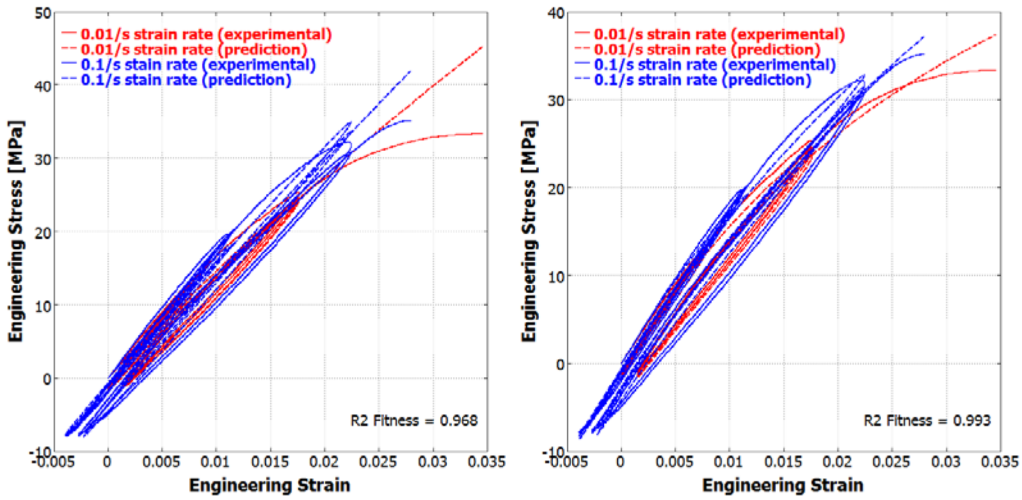

(a) **(b)**

Figure 4: Comparison between experimental results and (a) linear viscoelastic material model and (b) Parallel Network Model for Material 1.

Figure 5 shows the calibration results for Material 2. The viscoelastic material is calibrated up to only 5% strain, and shows, not surprisingly, a poor match to the experimental data. However, the 3- network model is capable of capturing the observed rate dependence and non-linear behaviour. It should be noted that this fit could be further improved with a greater number of experimental data points than those presented in Figure 2. The perturbations in the model prediction curves in Figure 5(b) are due to the small number of points used in discretising the input data.

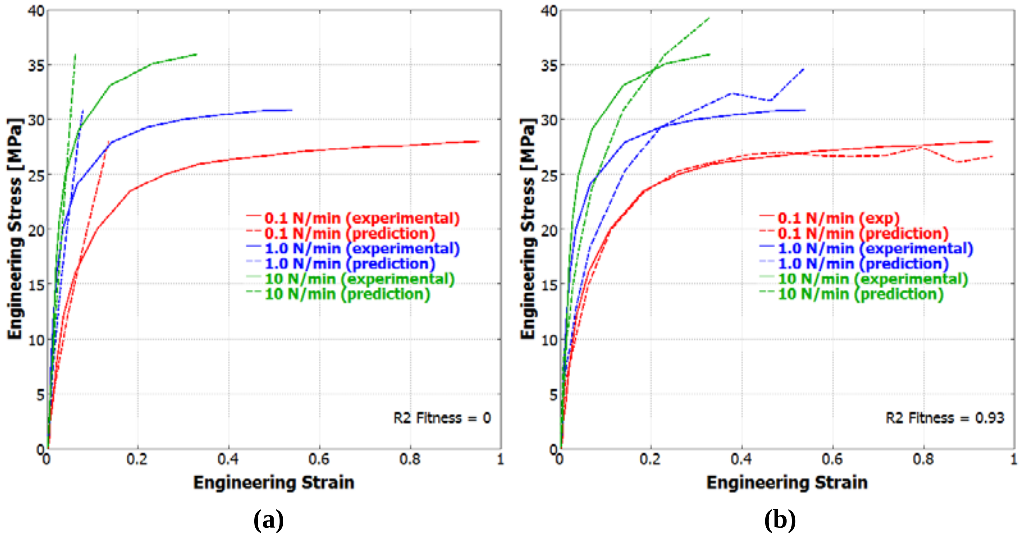

Figure 5: Comparison between experimental results and (a) viscoelastic material model and (b) Parallel Network Model for Material 2.

5: Finite Element Model of Drop Test

The calibrated material models were used to analyze the drop test performance of a biodegradable plastic casing for a generic smart phone using explicit nonlinear transient dynamic finite element analysis. The solid model and finite element mesh of the generic smart phone and protective case are shown in Figure 6. The model includes a biodegradable casing, the body of the phone, battery, LCD and floor. Contact conditions are established between the phone body and the case, and between the case and the floor. The phone is given an initial velocity of 5.5 m/s, which corresponds to a drop from 1.54 m. The floor is modelled as a stiff elastic surface with no energy dissipation and no dissipative boundaries. An explicit analysis is performed using Abaqus. The battery, LCD and floor are meshed with C3D8R elements, which are eight-node bricks with reduced integration and enhanced hour-glass control. The phone body and the casing are meshed with C3D10M elements, which are modified ten-node tetrahedral elements that are internally split into eight-node brick elements. A small amount of mass scaling is used to achieve a reasonable time step while only increasing the mass of the system by 0.2%. A penalty contact algorithm is used, as it is more suitable for multiple interacting contact surfaces and more efficient in multi-domain parallelization. The energy in the model due to viscous dissipation, mass scaling, penalty contact and hour-glass control are all monitored to ensure that they are insignificant compared to the strain energy, kinetic energy and energy lost due to material viscous effects and friction.

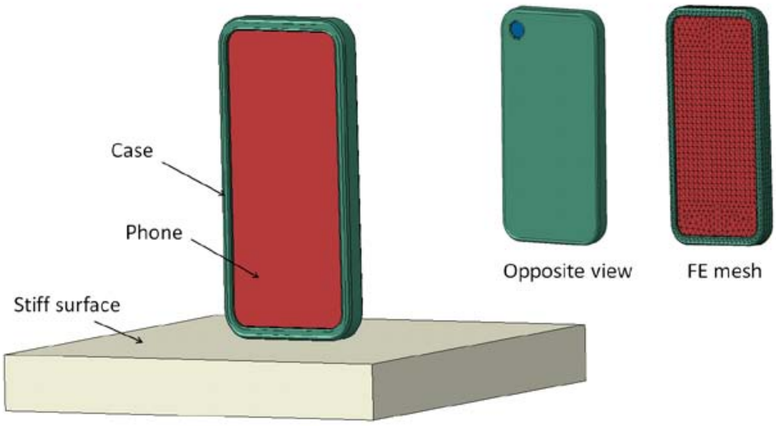

Figure 6: Model and finite element mesh used for the phone drop test.

6: Results

The efficacy of the casing in mitigating the damage to the phone is measured in terms of the total energy absorbed by the phone case during impact, the maximum strains in the phone case, and the maximum force transferred to the phone. Due to the lack of experimental data at high strain rates and the simplified phone model, only a qualitative assessment can be made regarding the stresses and strains that result from dropping the phone. Despite these limitations, a relative comparison of the material models presented can still be established. Furthermore, the overall framework used to evaluate material efficacy for a specific application is still applicable.

For Material 1, three simulations were performed to illustrate the effect of protective case material model on drop test results. The simulations use the following material models: (i) the calibrated viscoelastic model (LVE), (ii) the calibrated Parallel Network model (PNM-1), and (iii) the calibrated Parallel Network model without the third network responsible for high frequency damping (PNM-2). For Material 2, two simulations are performed using the calibrated Parallel Network model and the calibrated viscoelastic model. The viscoelastic simulation is performed for completeness even though this material model is clearly not suitable for Material 2. Figure 7 shows the maximum principal strain contours at three points in time for Material 1 using the Parallel Network model. Note that the impact between the protective casing and the ground starts at 0 ms, and ends at approximately 0.24 ms.

Table 1 summarizes the peak strains, energy dissipation (at 0.7 ms) and force transmission given by each material. For Material 1, both the three-element Parallel Network and the viscoelastic model capture the energy dissipation, and show the same general response. The lack of energy dissipation in the model without the high frequency damping network is further evidence of the need for high frequency components in any constitutive model used in drop testing simulations. For Material 2, there is a significant difference between the three-element Parallel Network and the viscoelastic model predictions.

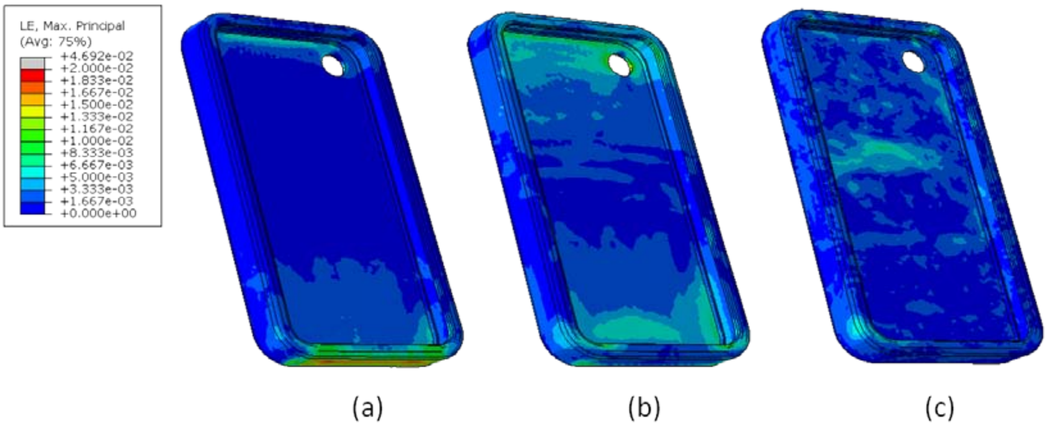

Figure 7: Maximum principal strain contours at (a) 0.1 ms, (b) 0.18 ms, and (c) 0.48 ms.

	Material 1: Pure PLA			**Material 2: PLLA + Plasticizer**	
Case	**LVE**	**PNM-1**	**PNM-2**	**LVE**	**PNM-1**
Maximum principal strain (%)	1.61	1.68	2.91	2.50	1.93
Viscous dissipation at 0.7 ms (J)	0.48	0.44	1.12×10^{-4}	0.79	0.57
Phone					
Maximum principal strain (%)	0.12	0.12	0.11	0.11	0.11
Peak transmitted force (kN)	6.56	6.47	5.66	8.31	5.98

Table 1: Summary of results

7: Conclusions

A material model was developed that accurately captures the constitutive behaviour of biodegradable polymers at high and low strains and strain rates. The model was calibrated to experimental data for two PLA-based plastics with different mechanical properties resulting from adding plasticizing additives. Using one constitutive modelling framework, we were able to predict the behaviour of the two significantly different materials. Finite element simulations of drop tests were performed for a generic smart phone protected by a biodegradable polymeric casing. The simulation results illustrate the effect of the casing material model on key drop test results such as total energy absorbed during impact, maximum force transmitted to the phone and strains in the case and phone. The developed material model, calibrated with the necessary experimental material test data, and together with an accurate phone drop model constitutes a valuable tool for consumer drop testing applications.

REFERENCES

1. Bergstrom, J.S., and Boyce, M.C., 1998, Constitutive modeling of the large strain time-dependent behavior of elastomers, *Journal of Mechanics and Physics of Solids*, 46, pp.931-954.

2. Bergstrom, J., Boyce, M.C., 2001, Constitutive modeling of the time-dependent and cyclic loading of elastomers and application to soft biological tissues, *Mechanics of Materials*, 33, pp.523-530.

3. Bergstrom, J., 2008, Dynamic finite element modeling of elastomers, 2008 Abaqus User Conference, Newport, RI, USA, May 208.

4. Bergstrom, J.S, Bischoff, J.E., 2010, An advanced thermomechanical constitutive model for UHMWPE, *International Journal of Structural Changes in Solids*, 2(1), pp.31-39.

5. Grabow, N., Martin, H. and Schmitz, K.P., 2002, The impact of material characteristics on the mechanical properties of a poly(L-lactide) coronary stent, *Biomedical Engineering*, 47, pp.503-505.

6. Grabow, N., Schlun, M., Sternberg, K., Hakansson, N., Kramer, S. and Schmitz, K.P., 2005, Mechanical properties of laser cut poly(L-lactide) micro-specimens: Implications for stent design, manufacture, and sterilization, *ASME Journal of Biomechanical Engineering*, 127, pp.25-31.

7. Graupner, N., Hermann, A.S., and Mussig, J., 2009, Natural and man-made cellulose fiber-reinfirced poly(lactic acid) (PLA) composites: An overview about mechanical characteristics and application areas, *Composites: Part A*, 40, pp.810-821.

8. Martin, O. and Avérouz, L., 2001, Poly(lactic acid): plasticization and properties of biodegradable multiphase systems, *Polymers,* 42, pp.6209-6219.

9. Ponkala, J.I., 2009, *On the design of a biodegradable POC-HA polymeric cardiovascular stent*, M.Sc. University of Texas at Arlington.

10. Soares, J.S., Moore Jr., J.E. and Rajagopal, K.R., 2008, Constitutive framework for biodegradable polymers with applications to biodegradable stents, *ASAIO Journal*, 54(3), pp.295-301.

11. Soares, J.S., Rajagopal, K.R. and Moore Jr., J.E. 2010, Deformation-induced hydrolysis of a degradable polymeric cylindrical annulus, *Biomechanics and Modeling in Mechanobiology*, 9, pp. 177-186.

12. Soares, J.S., 2008, *Constitutive modeling for biodegradable polymers for applications in endovascular stents*, Ph.D. Texas A&M University.

13. Veryst Engineering, 2010. *PolyUMod user-material model library* [online]. Available at <http://www.veryst.com/PolyUModLibrary.html>.